Mechanism comprehension and design of MOF catalysts for photocatalytic ammonia production

*Wengang Huang[1], Milton Chai[1, *], Rijia Lin[1], Vicki Chen[2] and Jingwei Hou[1, *]*

[1]*The School of Chemical Engineering, The University of Queensland, Brisbane, QLD 4072, Australia*

[2]*University of Technology, Sydney, 15 Broadway, Ultimo, NSW, Australia*

**Corresponding author.*

E-mail: milton.chai@uq.edu.au; Jingwei.hou@uq.edu.au

Abstract

Ammonia (NH_3) has attracted considerable attention as a source of fertilizer and a sustainable energy carrier. However, The Haber-Bosch ammonia manufacturing method continues to be plagued by excessive electrical consumption and carbon dioxide emissions. Alternatively, the photocatalytic production of NH_3 as an approach for N_2 fixation and solar energy conversion has been progressively demonstrated as a more benign synthesis strategy. Metal-organic frameworks (MOFs) as photocatalysts for ammonia production are becoming one of the most promising options due to their design flexibility and new form factors as composites. The goal of this Perspective paper is to offer a timely overview of recent advances in MOF catalysts for photocatalytic ammonia production, as well as an introduction to the fundamentals of N_2 fixation and the key state-of-the-art characterization for MOF catalysts. A detailed insight into the trend and challenges for MOF catalysts is also provided to stimulate inspiration in photocatalytic ammonia production.

Keywords: Nitrogen fixation, ammonia production, photocatalysis, MOF, catalyst

1. Introduction

Ammonia (NH_3) as an eco-friendly chemical is essential to natural life and industrial processes. Each year, hundreds of millions of tons of ammonia are produced and consumed in numerous industrial processes, including the production of fertilizers, pharmaceuticals, and explosives.[1] Moreover, with a high content of hydrogen, NH_3 as an ideal energy carrier exhibits a huge energy density. NH_3's volumetric energy density is 12.92-14.4 $GJ \cdot m^{-3}$, which is even higher than hydrogen and methanol.[2] Due to NH_3's stability and ease of transportation, it has come to be recognized as a safe alternative energy source to conventional fuels and hydrogen. At present, the Haber-Bosch (HB) is the most common method for manufacturing commercial ammonia (Figure 1A). This process's primary reaction can be depicted as: $N_2 + 3H_2 \rightarrow NH_3$, which involves high-pressure, high-energy consumption, and an expensive raw material, hydrogen. Given that increasing energy demand and rising carbon footprints pose the greatest challenge to contemporary society, it is crucial to produce ammonia in an eco-friendly and energy-efficient manner.

Photocatalytic production of NH_3 has attracted considerable research interest due to its ability to leverage limitless solar energy and produce NH_3 under mild conditions. Moreover, this technique has minimal environmental impact and is sustainable. Photocatalytic ammonia synthesis on semiconductors via nitrogen reduction reaction (NRR) requires multiple processes (Figure 1B). First, electron-hole pairs are produced by irradiating photocatalysts with light at energies higher than material's bandgap. The electrons then accumulate at the photocatalyst reaction sites where the NRR occurs. Significant research has been conducted to develop materials for photocatalytic NH_3 synthesis. Among these materials there have been semiconducting transition metal oxides, metallic-organic compounds, polymers, and carbon nitride. Nevertheless, their function as a photocatalyst faces several obstacles such as limited light capturing capabilities, short electron-hole pair lifetimes, weak electron transfer and limited active sites. Consequently, it is crucial to rationally design photocatalysts that satisfy all of these requirements.

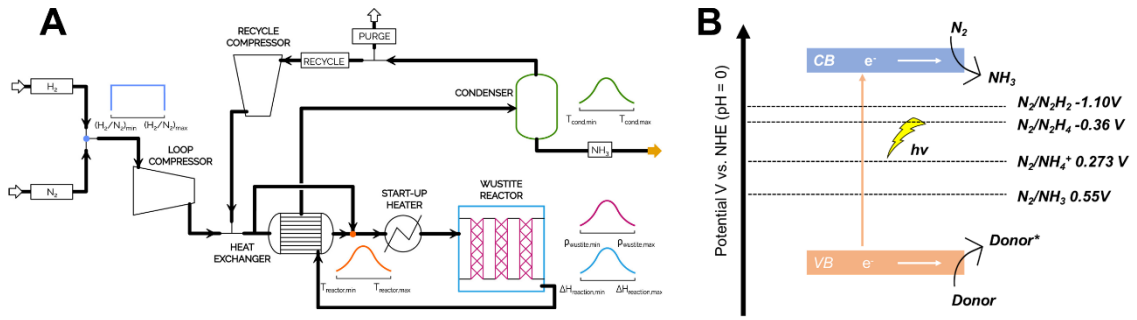

Figure 1. (A) Diagram of the Haber-Bosch process. Reprinted with permission from ref [3]. Copyright 2021 Elsevier. (B) Illustration of photocatalytic NH_3 production.

Metal-organic frameworks (MOFs) based catalysts have become one of the most prevalent choices for photocatalysis due to their facile synthesis and high structural/chemical tunability. As a family of coordination compounds made up of organic linkers and metal centers, MOFs are predominantly highly ordered porous materials with tunable pore sizes and with more research interest being shifted onto their amorphous family.[4-9] Materials based on MOFs have demonstrated considerable photocatalytic ability for a variety of reactions, including

photocatalytic production of hydrogen, H_2O_2, CO_2 reduction reaction, and removal of environmental pollutants.[10-12] Recent interest has also increased in light-driven NRR for ammonia synthesis catalyzed by MOFs. Compared to conventional transition metal oxides and carbon-based materials, MOFs stand out for photocatalysis NRR due to the following three benefits:[13-16] first, MOFs' porous structure and large surface area can enable a highly selective adsorption of nitrogen in their channels, assuring that the majority of electrons will transition from the excited MOF's active site to the N_2 molecules, thereby enhancing the photocatalytic efficiency. Secondly, the optical and electrical properties of MOFs are largely determined by their highly modifiable organic ligands. Functionalization of the linkers allows desirable bandgap and charge transfer rates to be achieved for NRR. Lastly, MOFs are the optimal matrix for compositing and engineering. It is possible to introduce defects or secondary metal clusters into MOF structures to achieve effective NRR. All these benefits can lead to the construction of MOF photocatalysts that may surpass the performance of conventional metal oxide photocatalysts for NRR. For example, a Ti-based MIL-125-NH_2 has substantially greater photocatalytic activity for nitrogen fixation under visible light irradiation than N-doped TiO_2.[17] Therefore, it is crucial to comprehend and rationally design MOF catalysts for more efficient photocatalytic ammonia production.

While there are a few studies which talk about how to design MOF for photocatalysis NRR, this Perspective paper will start with a concise introduction to the fundamentals of NRR and seeks to offer insights for designing and optimizing MOFs for the photocatalytic production of NH_3 from the perspectives of (1) linker functionalization, (2) defects engineering, and (3) MOF compositing. We also discussed the key but still under-utilized characterization techniques guiding the design of MOF catalysts. Finally, we shared our understanding and viewpoint regarding MOF photocatalytic NH_3 production.

2. Fundamentals of the NRR

Enzymatic nitrogen reduction reaction has been regarded as a key process in the earth's ecosystem since it accounts for nearly 90% of natural NRR during the past million years.[18] Molybdenum (Mo)-dependent enzyme, with FeMo active-sites, is the most well-investigated enzyme for NRR mechanism.[19, 20] This enzyme accumulates protons and electrons before the adsorption of dinitrogen on the enzyme's active site. Subsequently, in the presence of dinitrogen, protons are partially reduced to dihydrogen and then get eliminated for N_2 coordination reaction.[21, 22] There are two pathways as depicted in Figure 2A in which enzymatic NRR can take place, i.e., the distal and alternating pathway. In the distal pathway, the remote nitrogen atom gets reduced to ammonia prior to the other one; while in the alternating pathway, dinitrogen attaches on the active site and both N atoms are simultaneously reduced.[23]

Similar to the enzyme catalysts, the industrial HB process also employs transition metal-based synthetic catalysts to produce NH_3. The mechanistic pathways of the synthetic catalysts include an associative or dissociative mechanism. In an associative mechanism, dinitrogen molecules are adsorbed on the surface of the heterogeneous catalyst in an end-on mode, where the N–N bond is cleaved simultaneously with the release of the first molecule of ammonia. Both the distal and the alternating pathways described in Figure 2B are variations of an associative pathway. The other is the dissociative mechanism (Figure 2B top), where $N \equiv N$ bond is dissociated into N radicals or N atoms before hydrogenation. Catalysts then adsorb N radicals (atoms) on the surface for the hydrogenation process.[23, 24]

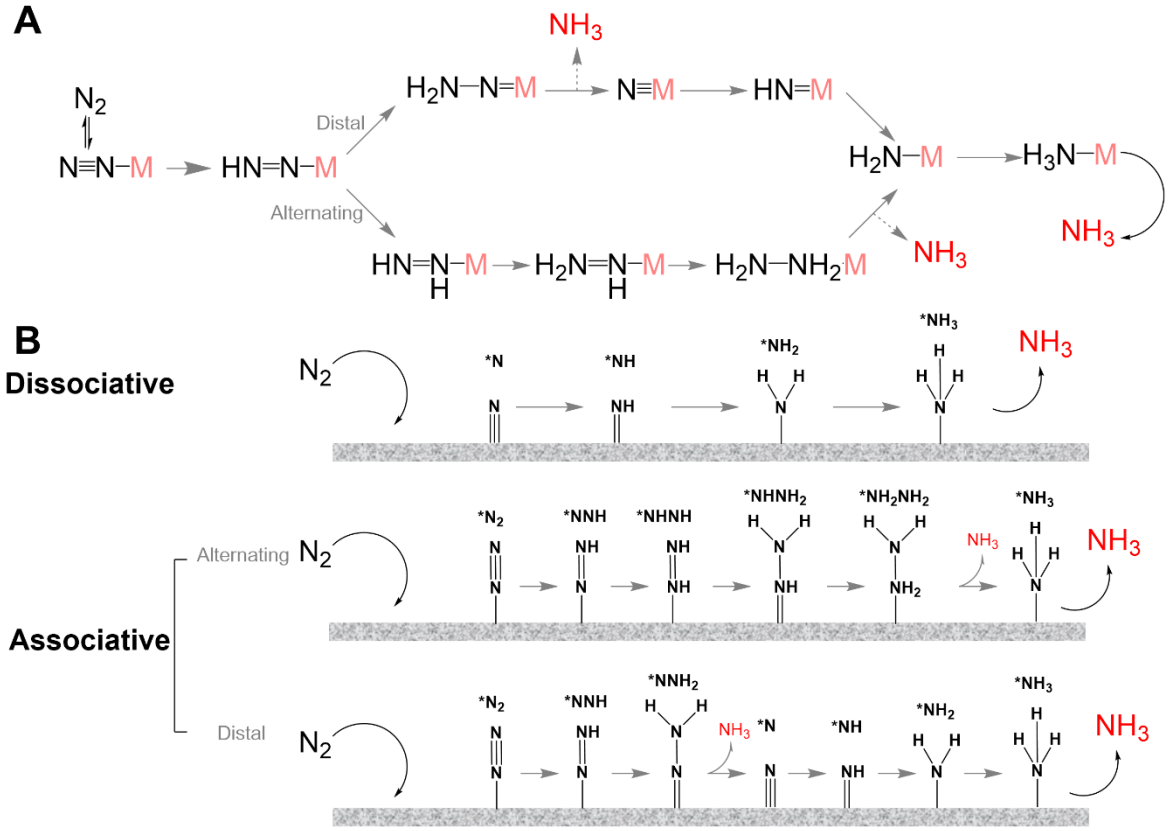

Figure 2. (A) Enzymatic pathway for NRR. (B) Mechanisms for the two pathways of NRR using synthetic catalysts.

The photocatalytic NRR involves three steps: (1) light absorption for photo-generation of electrons, (2) charge separation and (3) participation of electrons in the surface NRR. Generally, when a photocatalyst is irradiated by photons with energy greater than its band gap, there will be electrons excited from the valence band (VB) to the conduction band (CB), and leave a hole at VB. Then, the hole can be quenched by a sacrificial agent (VB should be more positive than the sacrificial agent's redox potential) while dinitrogen can be reduced by electrons (CB should be more negative than dinitrogen hydrogenation potential). The dinitrogen hydrogenation potentials are summarized in Table 1.

Table 1. The dinitrogen hydrogenation potentials (*vs*. NHE at pH 0)

Reduction reaction	E^0 (V)
$N_2 + e^- \rightarrow N_2^-$	-4.2
$N_2 + H^+ + e^- \rightarrow N_2H$	-3.2
$N_2 + 6H^+ + 6e^- \rightarrow 2NH_3$	0.55
$N_2 + 8H^+ + 8e^- \rightarrow 2NH_4^+$	0.27

The actual reaction pathway of NRR at the active site of a photocatalyst is extremely complex and might involve multiple pathways. The coordination environment of the active site will undoubtedly influence the NRR reduction pathways. Therefore, we believe it would be

advisable to combine experimental investigation and computational simulation to comprehend the NRR case by case.

3. Insight into the design and tuning of MOF photocatalysts

Why MOFs?

During the past decade, numerous visible-light photocatalysts have been developed for ammonia production which included WO_3/CdS heterojunction,[25] doped TiO_2,[26] and modified Layered Double Hydroxide (LDH).[27] These inorganic materials exhibited high physical and chemical stability; for instance, a modified LDH designed by Zhang et al. can produce ammonia continuously for more than 40 hours under continuous light irradiation.[28] In all of these investigations aimed at developing efficient visible-light photocatalysts, there have been two major obstacles: (1) to reduce their absorption energy below 3 eV so that photocatalysis can be performed under visible light, and (2) to separate photogenerated electrons and holes by minimizing their immediate recombination, allowing these photogenerated carriers to initiate nitrogen reduction reaction.[29] In contrast, MOFs, despite still facing challenges in stability and efficiency, are showing potential for circumventing these two obstacles: firstly, the organic ligands such as benzene derivatives would allow them to absorb visible light; and secondly, the intimate contact between organic linkers and metal nodes could be advantageous for charge separation. Given the nearly infinite number of possible metal nodes/clusters and organic linker combinations, MOFs exhibit a wide range of structural and chemical variability, making them excellent candidates for photocatalysis ammonia production. However, low conductivity, instability, and charge recombination are still MOF's main bottlenecks for achieving desirable levels of photocatalytic ammonia production.[15] To address these challenges, we focus on MOF's design flexibility and report their recent advances in solar-driven ammonia production. This section highlights the design and tuning of MOF-based photocatalysts for enhanced ammonia production from the following perspectives: (1) organic linker functionalization in MOFs, (2) defect engineering in MOFs, and (3) MOF compositing strategy.

3.1 Organic linker functionalization in MOFs

Linker functionalization has been widely employed for modifying the physical and chemical characteristics of MOFs, and it also serves as an efficient method for improving the optical properties of MOFs.[30, 31] For example, the optical properties and nitrogen fixation ability of a Ti-based MOF (MIL-125) was found to be linearly associated with the light-harvesting efficiency of ligands' functional groups.[17] Figure 3A-C demonstrate that incorporation of amine-functionalized linkers with highly efficient visible light harvesting capability, such as the H_2BDC-NH_2 (2-aminoterephthalate), harvested more visible light and therefore can generate more photoexcited electrons for NRR upon illumination while maintaining a similar crystal structure as pure MIL-125. The light harvesting functional group is highlighted in red in Figure 3D.

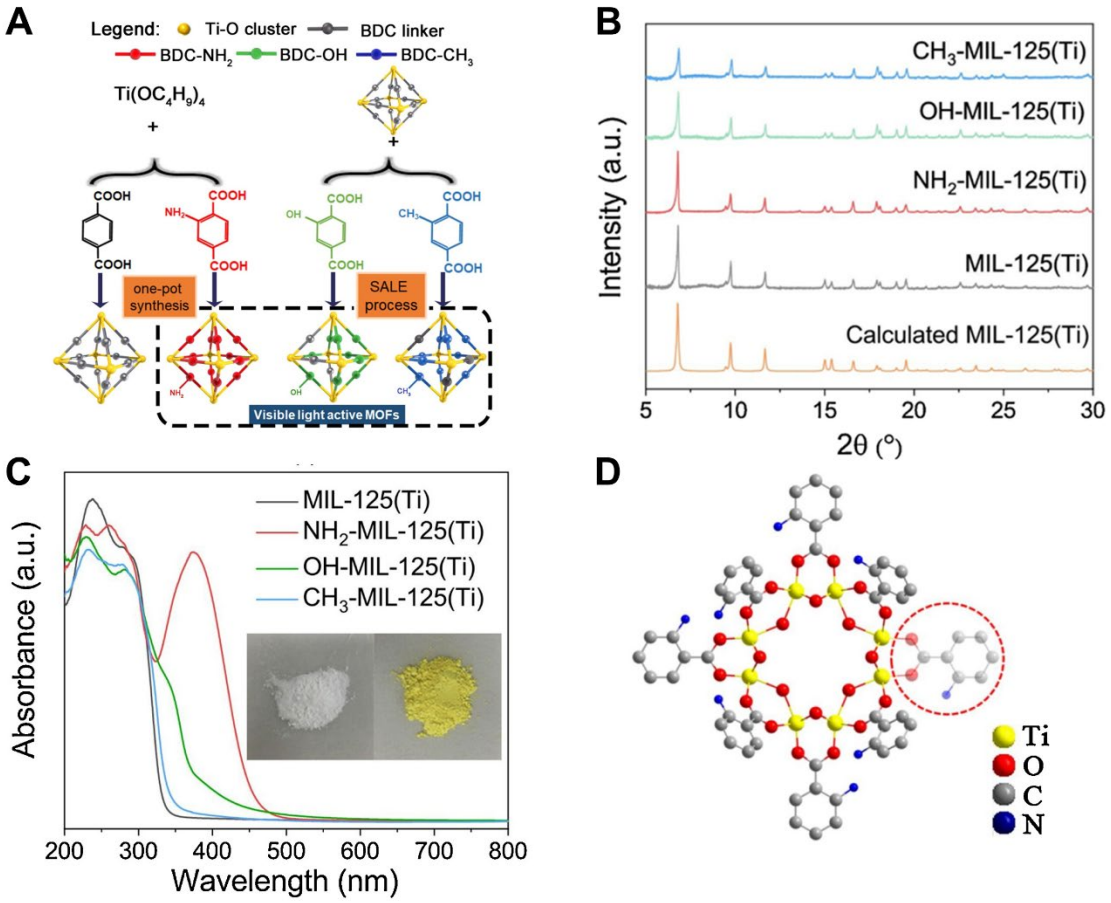

Figure 3. (A) Linker functionalization for MIL-125 (Ti). (B) Comparison of powder X-ray diffraction (PXRD) patterns for functionalized MOF series. (C) Linker functionalization enables NH_2-MIL-125 to harvest visible light. (D) Light harvesting site in NH_2-MIL-125. Reprinted with permission from ref [17]. Copyright 2020 Elsevier.

In addition to the widely used amine functional group, other types of functionalized linkers have also been explored to improve the light-harvesting ability of MOF for ammonia production. Jiang et al. have recently reported that the introduction of two thiol groups (SH) in the linkers of U(Zr-Hf)-SH enabled it to absorb visible light.[32] Variations of the functional groups on the linkers in U(Zr-Hf)-X (X = 2SH, OH, Cl) did not change the crystal structure, although their displayed morphology and light absorbance were different (Figure 4A-C). Among the different functional groups tested, U(Zr-Hf)-SH exhibited a substantially higher NRR rate, reaching 116 μmol g^{-1} h^{-1} under visible light, which was associated with the optimal electron transfer pathway (Figure 4D-E). Figure 4F illustrates the proposed mechanism of NRR for U(Zr-Hf)-SH. Initially, when irradiated by visible light, the SH functionalized ligand absorbs solar energy, leading to the creation of electron-hole pairs. Subsequently, the holes are quenched by the sacrificial agent K_2SO_3, while the electrons occupy the Lowest Occupied Molecular Orbital. The electrons undergo further absorption of solar energy, transitioning to a higher excited state with an energy level of -3.29 eV. In the next step, these excited electrons migrate from the ligand to the metal-oxygen cluster due to the relatively higher potentials of Hf-O and Zr-O. The electrons ultimately migrate from the metal-oxygen complex to the activated N_2, which facilitates the formation of ammonia.

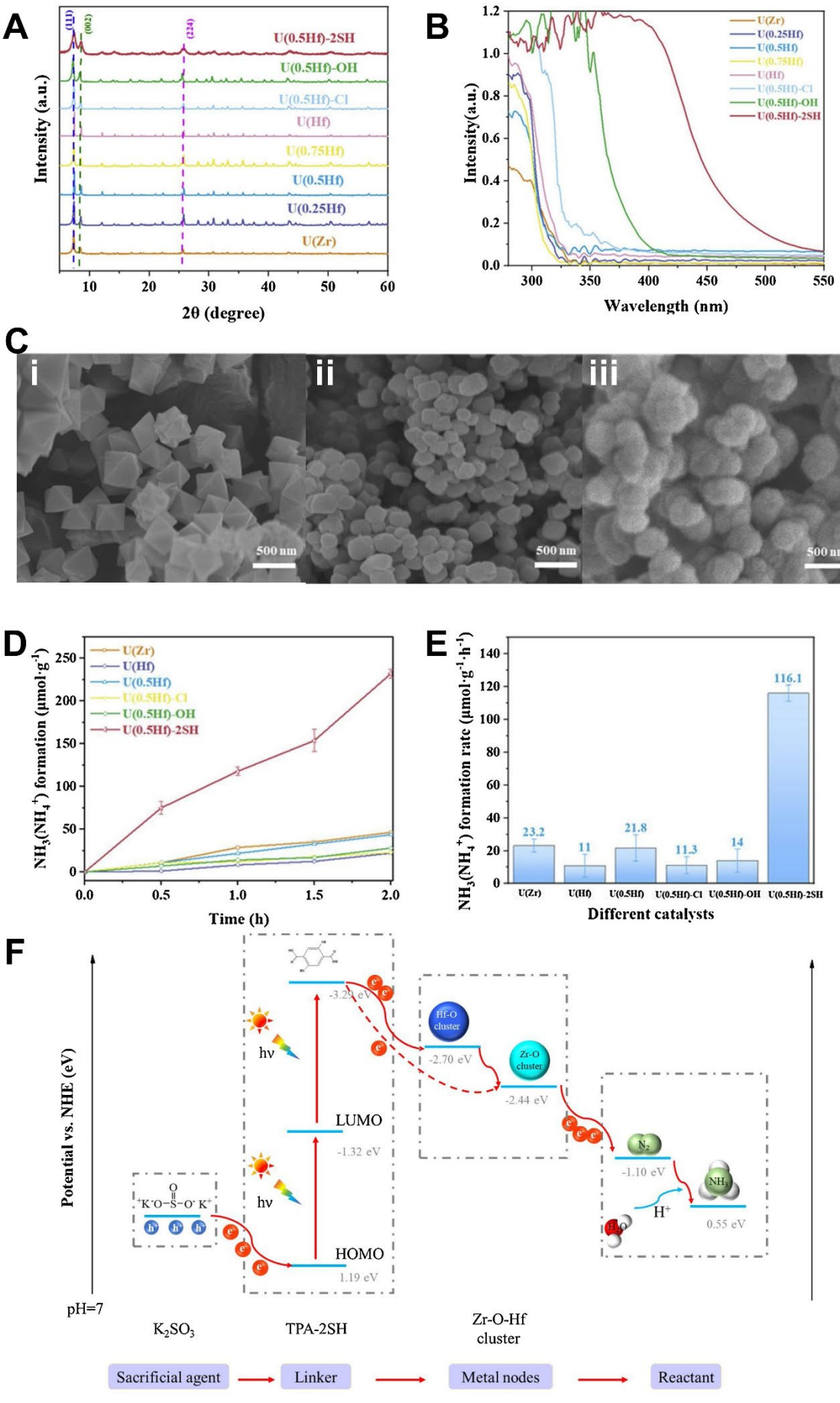
A
(111)
(002)
(224)
U(0.5Hf)-2SH
U(0.5Hf)-OH
U(0.5Hf)-Cl
U(Hf)
U(0.75Hf)
U(0.5Hf)
U(0.25Hf)
U(Zr)
Intensity (a.u.)
2θ (degree)
B
U(Zr)
U(0.25Hf)
U(0.5Hf)
U(0.75Hf)
U(Hf)
U(0.5Hf)-Cl
U(0.5Hf)-OH
U(0.5Hf)-2SH
Intensity(a.u.)
Wavelength (nm)
C
i
ii
iii
500 nm
D
U(Zr)
U(Hf)
U(0.5Hf)
U(0.5Hf)-Cl
U(0.5Hf)-OH
U(0.5Hf)-2SH
NH3(NH4+) formation (μmol·g-1)
Time (h)
E
NH3(NH4+) formation rate (μmol·g-1·h-1)
23.2
11
21.8
11.3
14
116.1
U(Zr)
U(Hf)
U(0.5Hf)
U(0.5Hf)-Cl
U(0.5Hf)-OH
U(0.5Hf)-2SH
Different catalysts
F
Potential vs. NHE (eV)
pH=7
hν
LUMO
-1.32 eV
HOMO
1.19 eV
-3.29 eV
Hf-O cluster
-2.70 eV
Zr-O cluster
-2.44 eV
N2
-1.10 eV
NH3
0.55 eV
H+
H2O
K2SO3
TPA-2SH
Zr-O-Hf cluster
Sacrificial agent
Linker
Metal nodes
Reactant

Figure 4. U(Zr-Hf)-X characterization and ammonia production comparison (X = Cl, OH, SH). (A) PXRD patterns. (B) UV–vis spectrum. (C) SEM images of U(Zr-Hf)-X. (D) NH_3 evolution curves (E) Corresponding NH_3 evolution rates over different functional groups. (F) The mechanism for the NRR over U(Zr-Hf)-2SH. Reprinted with permission from ref [32]. Copyright 2021 Elsevier.

Post-synthetic modification of organic linkers is an alternative technique for enhancing photocatalytic NRR activity. The implementation of the Schiff base reaction between the amino group or aldehyde group of an organic linker is a common strategy.[33] It enhances the conjugation systems inside the highly ordered crystal structure and thus improves the light absorbance ability. Moreover, the incorporation of 2-pyridinecarboxaldehyde with amino-functionalized linkers can form an imino-pyridine structure, which offers opportunities for anchoring an electron mediator such as Rh-complex or Ru-complex. Therefore, linker functionalization of MOFs could be an effective approach not only for enhancing the light-harvesting capability, but also for achieving NRR through the incorporation of desirable sensitizers or mediators.

3.2 Defect Engineering in MOFs

Structural defects in a coordination network, such as a modified metal cluster, vacancy, disorder/dislocation or a missing linker, can alter the channel structure and physiochemical properties of the parent framework.[34, 35] Metal doping is a common strategy for modulating the structural, optical, and chemical properties of MOF-based semiconductors. To achieve activation of nitrogen, Zhang et al. introduced Cu into MIL-101(Fe) for the first time.[36] According to their PXRD results, all x-Cu-MIL-101(Fe) and MIL-101 (Fe) exhibit similar patterns except for one main peak (ca. 8° ~ 10°) that was shifted to a smaller angle, implying that the doped Cu altered the lattice structure (Figure 5A). A stronger reducibility for NRR was achieved by Cu-MIL-101(Fe) as Cu makes the CB more negative (-0.7 eV for Cu-doped material compared to -0.13 eV for pristine material). Consequently, a nitrogen fixation activity of approximately 315 $\mu mol \cdot h^{-1} \cdot g^{-1}$ was achieved by this strategy, three times higher than unmodified samples. Yan et al. adopted a similar strategy, as depicted in Figure 5B, in which a series of MOF-74 modified with Ru was designed for NRR.[37] The incorporation of Ru into MOF-74 not only reduced crystallinity but also stimulated the development of crystal planes between 35° and 38° (Figure 5B). Enhanced light-harvesting ability was also achieved due to narrowing of the bandgap by Ru doping.

Apart from metal doping, linker defects have also been proven to be effective for photocatalytic NRR. Luo et al. discovered that the ligand defects on UiO-66 induced by UV light irradiation can significantly enhance the NRR performance (Figure 5C). In contrast to the PXRD of pure UiO-66, defective samples exhibit a broad peak in the low-angle region, which is indicative of missing linker defects. The NRR performance increases from 125 $\mu mol\ g^{-1}\ h^{-1}$ for the pristine sample to 198 $\mu mol\ g^{-1}\ h^{-1}$ for the defective samples due to the formation of unsaturated metal nodes as a result of linker defects.[38] Linker defects can also facilitate substrate (N_2) diffusion. Guo et al. dehydrated UiO-66(SH) to form linker defects around the metal core cluster (Figure 5D). The sample treated at high temperature achieved an ammonia generation rate of approximately 32 $\mu mol\ g^{-1}\ h^{-1}$, which is seven times that of the untreated sample. Linker defects were found to open a "gate" for the diffusion of N_2 into the metal cluster, where dinitrogen molecules were then cleaved by unsaturated metal nodes.[39]

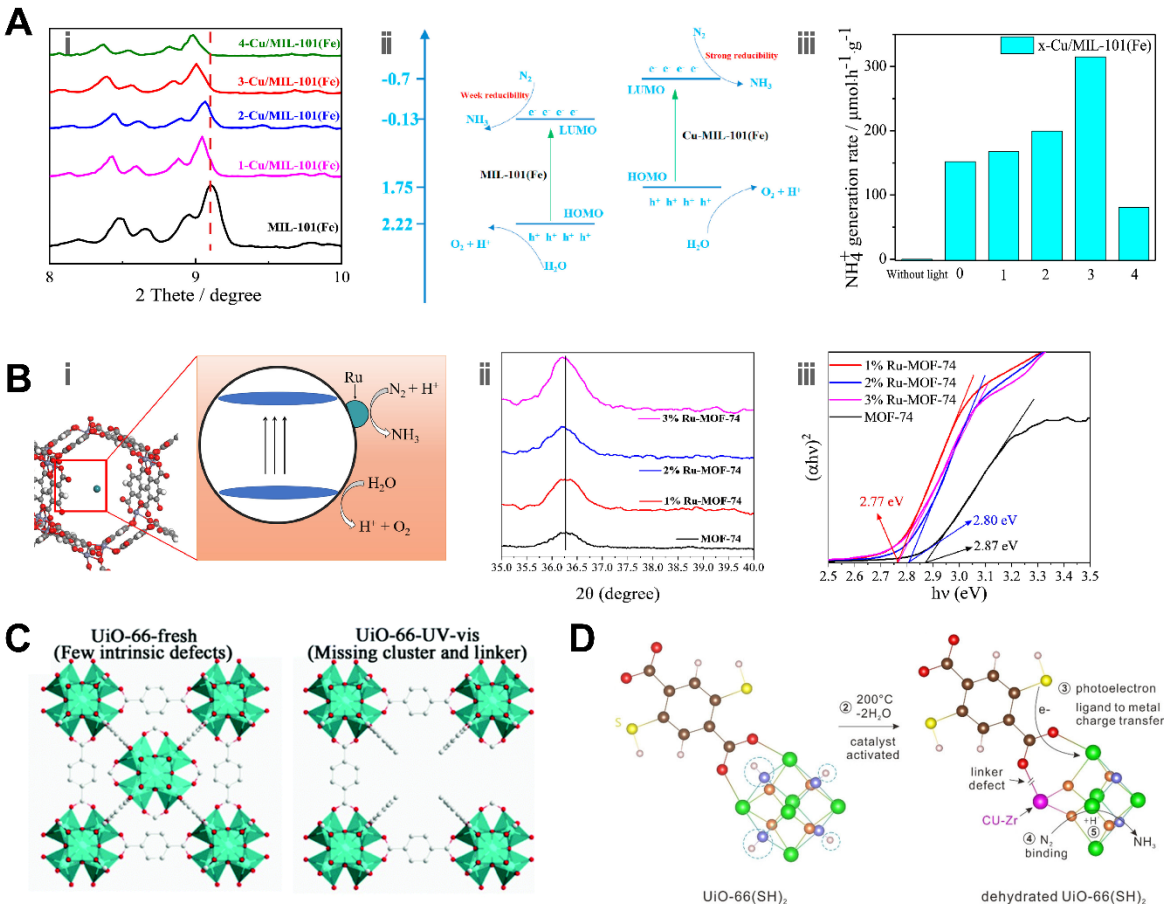

Figure 5. (A) PXRD patterns of x-Cu-MIL-101(Fe) and MIL-101 (Fe): (i) PXRD patterns. (ii) Bandgap structure. (iii) Ammonia productivity. Reprinted with permission from ref [36]. Copyright 2022 Elsevier. (B) Doping Ru in MOF-74 for enhancing NRR: (i) NRR mechanism for Ru-MOF-74 (ii) XRD patterns of the series of Ru-MOF-74 (iii) Energy bad gaps for the series Ru-MOF-74. Reprinted with permission from ref [37]. Copyright 2022 Elsevier. (C) Illustration of the crystal defects induced by UV irradiation. Reprinted with permission from ref [38]. Copyright 2021 Royal Society of Chemistry. (D) Local structure of UiO-66(SH) before and after dehydration. Reprinted with permission from ref [39]. Copyright 2022 Wiley-VCH.

It is apparent that introducing defects is an effective method for improving substrate diffusion, lowering the N_2 activating energy, and boosting photocatalytic activity. Nonetheless, the density of introduced defects should be optimized, as an excessive introduction reduces the light-harnessing ability and MOF's stability. Another technique for defect engineering should also be mentioned is amorphization, which is rarely explored for improving MOF photocatalysts, though it is widely used for enhancing photocatalysis efficiency of transition-metal oxide materials.[40] Metal centers in crystal MOFs are relatively difficult to modify given that they are highly coordinated. Amorphous MOFs, on the other hand, which retain the essential short-range building blocks yet lacking long-range order, offer an abundance of accessible metal sites for catalysis. For example, our group designed a bimetallic MOF glass obtained by sintered ZIF-62(Co) and $Fe(acac)_3$ (Figure 6).[41] During melting, ZIF-62(Co) forms a dense MOF liquid with a large number of uncoordinated N sites, which react with the Fe metal ions to produce Fe-N bonds. These Fe-N bonds remain in the bimetallic MOF glass after the quenching procedure and exhibit enhanced catalysis capacity. Therefore, consideration

should also be given to these amorphous MOF structures, which can offer a large number of uncoordinated sites. A subgroup of them can display melting or glass transition behaviour, thereby facilitating device fabrication.

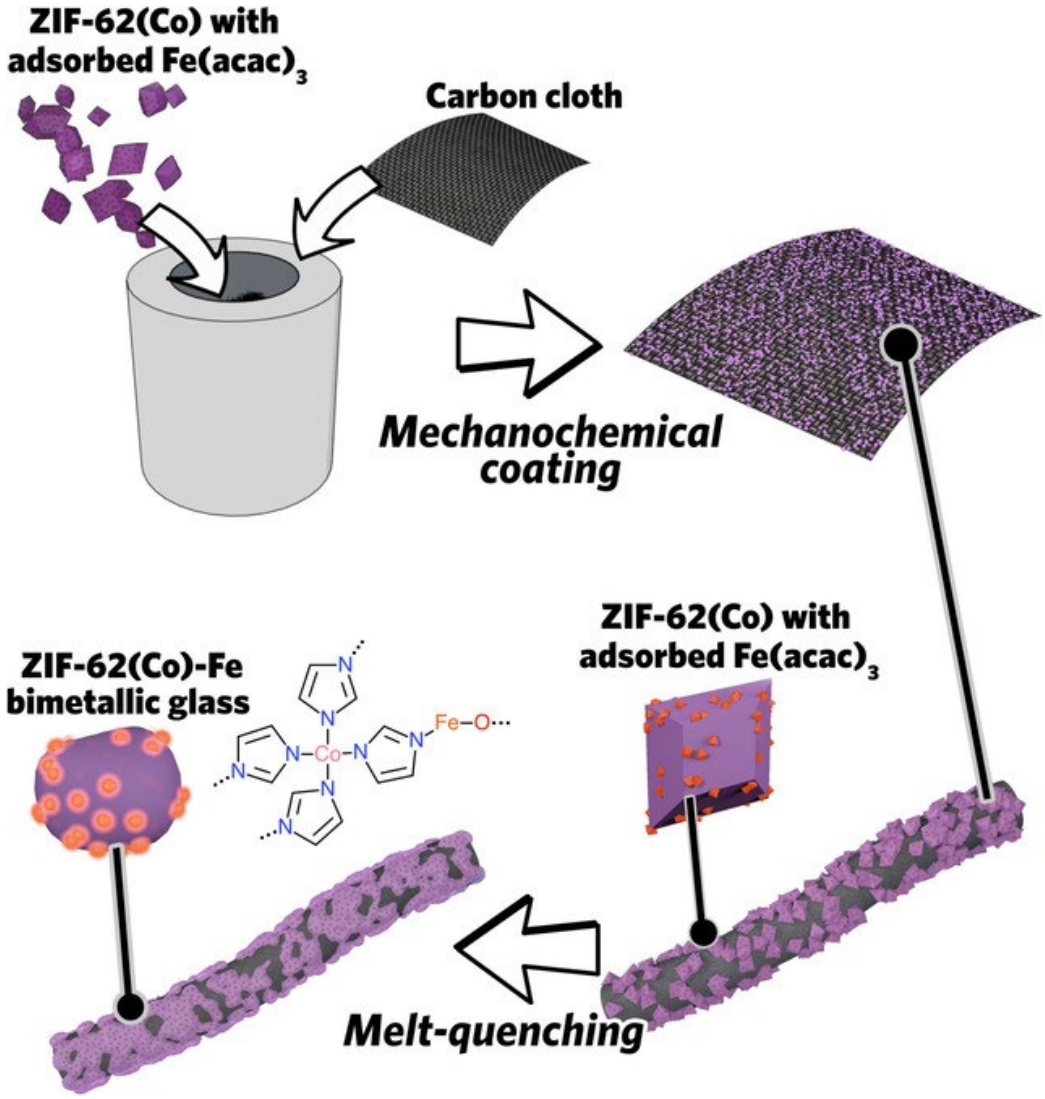

Figure 6. Amorphization ZIF-62(Co) with $Fe(acac)_3$ for enhanced catalysis performance. Reprinted with permission from ref [41]. Copyright 2021 Wiley-VCH.

3.3 MOF composite for photocatalytic ammonia production

Instead of functioning as a sole photocatalyst for NRR, the compounding of MOFs with co-catalysts and other semiconductors is an appealing technique of improving photoexcited carrier lifetime and enhancing NRR activity. MOF's well-defined channels, high surface area with abundant active sites, along with potential functional groups on organic ligands all enable the stable immobilization of nanoparticles, co-catalyst, and even perovskite.

Polyoxometalates

The incorporation of additional metal ions or metal clusters into the crystal structure of MOFs can endow them with unanticipated properties. Polyoxometalates (POMs) have been considered as promising photocatalysts in light of their unique band structure and active metal sites, nevertheless, their stability has always been criticized. Recent studies have emphasized the hybridization of polyoxometalates and metal-organic frameworks (MOFs), as some MOFs can entrap POMs and protect them from the ambient environment. Li et al. revealed that the combination of POMs and ZIF-67 improved the stability and photocatalytic activity of NRR (Figure 7A).[42] In comparison to pure ZIF-67 or POMs, the composite exhibited enhanced stability and catalytic activity. This is due to the porous structure of ZIF-67, which not only acted as a N_2 adsorbent but also served as a protective layer for the stabilization of POMs. The photoexcited electrons are able to be transferred from POMs to ZIF-67, and eventually the adsorbed N_2 molecules. A similar strategy was also adopted by Su et al (Figure 7B).[43] A series of POMs (SiW_{12}) supported in MIL-101(Cr) were synthesized, and the optimized NRR rate of over 75$\mu M \cdot h^{-1} \cdot g^{-1}$ was obtained as a result of the synergistic effect between their POMs and MOFs. Based on these reports, the integration of POMs cluster into MOFs contributes to enhanced photocatalytic NRR in terms of the addition of new metal sites, the enhancement of visible light absorption, the improvement of the materials' stability, the efficient inhibition of carrier recombination, and the mitigation of charge-transfer impedance.

Plasmonic nanoparticles

The incorporation of plasmonic nanoparticles in photoactive MOFs is extremely sought after due to plasmonic near field enhancement, complementary light absorption, and enhanced separation of electron-holes at the junction interface.[44] Not only are the functionalities of the individual components retained, but the synergistic effects between components also provide improved physiochemical properties.[45] Recently Chen et al. utilized UiO-66 to encapsulate Au nanoparticles (AuNPs) for plasmonic photocatalytic NRR.[46] The porous UiO-66 not only served as a matrix for Au nanoparticle confinement but also allowed their exposure to dinitrogen and protons for NRR (Figure 7C). While the majority of heterogeneous NRR reactions involve suspended particles, the Au@UiO-66 has been dispersed on a PTFE membrane for membrane reactor construction. This allowed for the direct introduction of N_2 to one side of the membrane while water and protons were introduced to the opposite side. This approach addresses the limited solubility and slow diffusion of N_2 in aqueous solutions, thereby improving the productivity and adaptability of NRR processes.

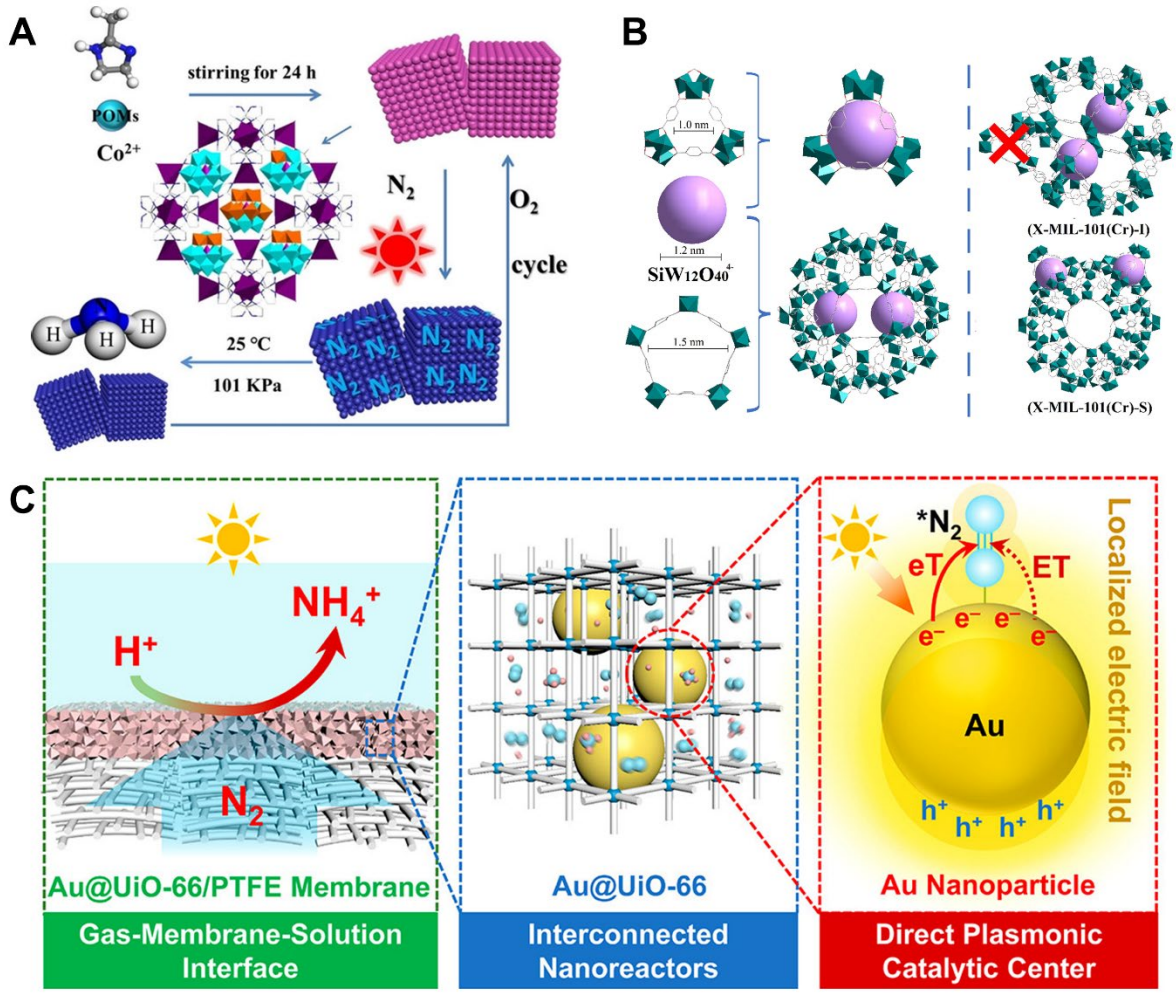

Figure 7. (A) Schematic illustration of the preparation of POMs@ZIF-67 and application in photocatalytic NRR. Reprinted with permission from ref [42]. Copyright 2020 Wiley-VCH (B) Schematic illustration of the POM encapsulated in MIL-101(Cr). Reprinted with permission from ref [43]. Copyright 2022 Elsevier. (C) Schematic illustration of the membrane reactor based on Au@UiO-66 for NRR. Reprinted with permission from ref [46]. Copyright 2021 American Chemical Society.

Perovskite

Evidence from a number of studies has established that perovskite and MOF hybridization can play noteworthy roles in photocatalytic NRR. Owing to their proper band structure, several types of perovskites have been investigated for effective NRR, such as $KNbO_3$, $LaCoO_3$, $SrTiO_3$, and $BiFeO_3$.[47-49] However, low surface area and weak interactions between nitrogen gas molecules and the surface atoms of solid perovskite restricted their photocatalytic NRR efficiency.[50] Existing research recognizes the critical role played by MOF in a MOF-perovskite composite photocatalyst.[51] Liu et al. prepared a $Bi_4O_5Br_2$/ZIF-8 photocatalyst by co-precipitation.[51] Compared with the pure perovskite, the composite $Bi_4O_5Br_2$/ZIF-8 (30%) exhibited significant improvement in photocatalytic NRR performance (327.338 $\mu M \cdot h^{-1} \cdot g^{-1}$, the efficacy has increased by over threefold) due to direct delivery of N_2 from air to the photocatalytic reaction interface (a triple-phase interface) established by the hydrophilic-hydrophobic structure of $Bi_4O_5Br_2$/ZIF-8 (Figure 8A). The formation of a heterostructure by

MOF and perovskite is also effective for NRR. According to Chamack et al., the hybridization of $KNbO_3$ and TMU-5 (Figure 8B) achieved an NH_3 production rate approximately 1.5 times that of pure perovskite (39.9 $\mu M \cdot h^{-1} \cdot g^{-1}$ upon ultra-violet irradiation for $KNbO_3$@TMU-5 compared to 20.5 $\mu M \cdot h^{-1} \cdot g^{-1}$ for $KNbO_3$ only).[50] TMU-5 in the heterostructure showed a high affinity towards Nb and improved the material's surface area for N_2 diffusion leading to enhanced NRR.

Moreover, glassy MOF-perovskite composite, which was first introduced by our group, also exhibited tremendous potential for photocatalytic NRR (Figure 8C).[52] Metal halide perovskite, such as $CsPbI_3$, can form a photoactive black phase upon heating, and the bandgap of this black phase is suitable for NRR. Nevertheless, thermodynamic factors tend to drive it to an undesired inactive yellow phase at ambient temperature. Glassy MOF a_gZIF-62 can stabilize the black phase of this perovskite at room temperature through interfacial interactions. The porous glassy MOF-perovskite composite can protect perovskite against external moisture and temperature stimuli while retaining their optical properties, which presents great potential as a photocatalyst for NRR application.

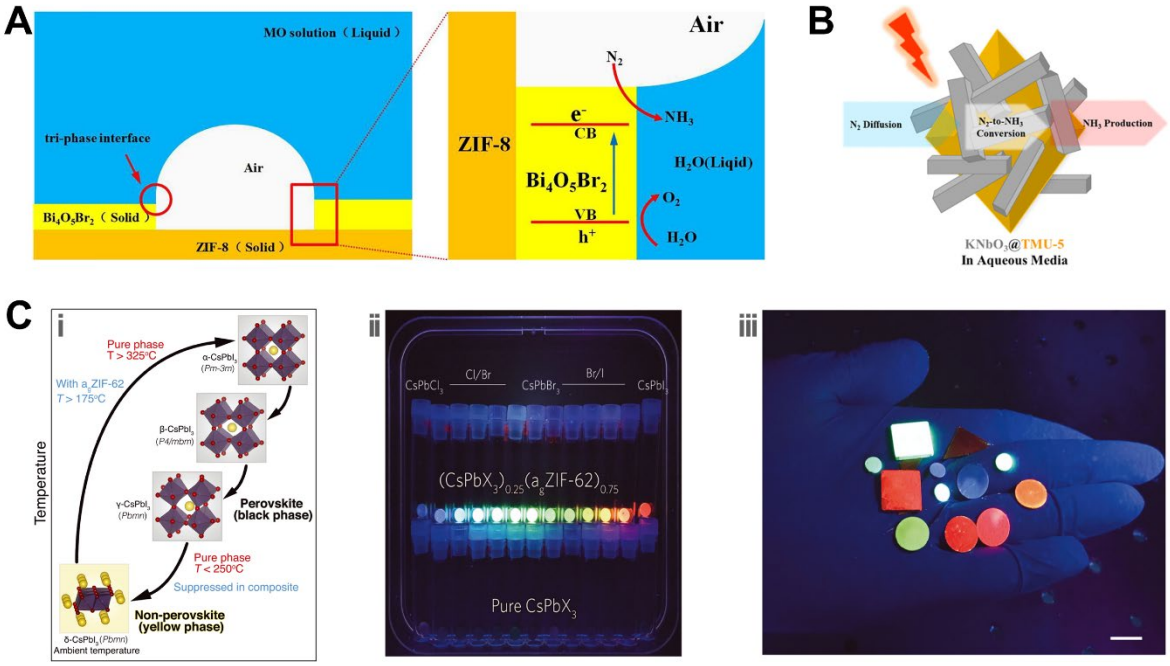

Figure 8. (A) Triple-phase interface established by MOF-perovskite composite. Reprinted with permission from ref [51]. Copyright 2019 Elsevier. (B) Schematical illustration of heterostructure $KNbO_3$@TMU-5. Reprinted with permission from ref [50]. Copyright 2022 American Chemical Society (C) MOF glass-perovskite composite fabrication. (i) Phase transition of $CsPbI_3$ upon heating and cooling. (ii) Optical properties of the composites and pure $CsPbX_3$ under UV illumination. (iii) Black phase perovskite's optical properties retained in glassy MOF. Reprinted with permission from ref [52]. Copyright 2021 AAAS.

MOFs and glassy MOFs exhibit relatively higher resistance to most polar solvents, enabling them to serve as scaffolds or functional interlayers to considerably enhance the robustness and photocatalytic ability of perovskite crystals. Furthermore, the high surface area of MOF promotes interfacial contacts between perovskite crystal and the electron mediators, which

facilitates electron extraction and mitigates charge recombination for enhanced photocatalytic NRR performance.[53]

4. Insight from advanced material analytical methods

Understanding the active sites and functional components of MOFs will assist and facilitate the design and tuning of MOF catalysts. Short-range/local probes including X-ray photoelectron spectroscopy (XPS) and electron microscopy can be utilized to determine MOF's chemical state of elements, but they cannot provide details on the atomic level such as explicit coordination environment and electronic properties of the active site or introduced component. Within this context, the pressing need for advanced characterization and advanced analysis techniques has led to significant advances in the field of MOF photocatalytic NRR.

4.1 XAS: Probing Atomic Structure

X-ray absorption spectroscopies (XAS) is an effective technique for probing the atom's local electronic structure as well as atom's coordination environments in a MOF structure. X-ray absorption near-edge structure (XANES) can reveal the state of atom, while the extended X-ray absorption fine structure (EXAFS) can probe atom's bond distances of neighbor atoms and coordination number. For instance, Shang et al. reported a porphyrin-based MOF Al-PMOF(Fe) with atomically dispersed Fe metal for photocatalysis NRR (Figure 9A).[54] To gain insight into the function of Fe, XAS was conducted for explicit structural analysis (Figure 9B-D). The EXAFS spectra confirmed the atomically dispersed Fe ions, meanwhile, the fitting results provide details for Fe–N bonding parameters, including bond distance and coordination numbers. Combining XAS and electrochemical results, the authors discovered that Fe insertion into the porphyrin ring of the MOF, which functions as the primary charge carrier acceptor, inhibits electron–hole coupling effectively, thereby enhancing the photocatalytic activity of NRR.

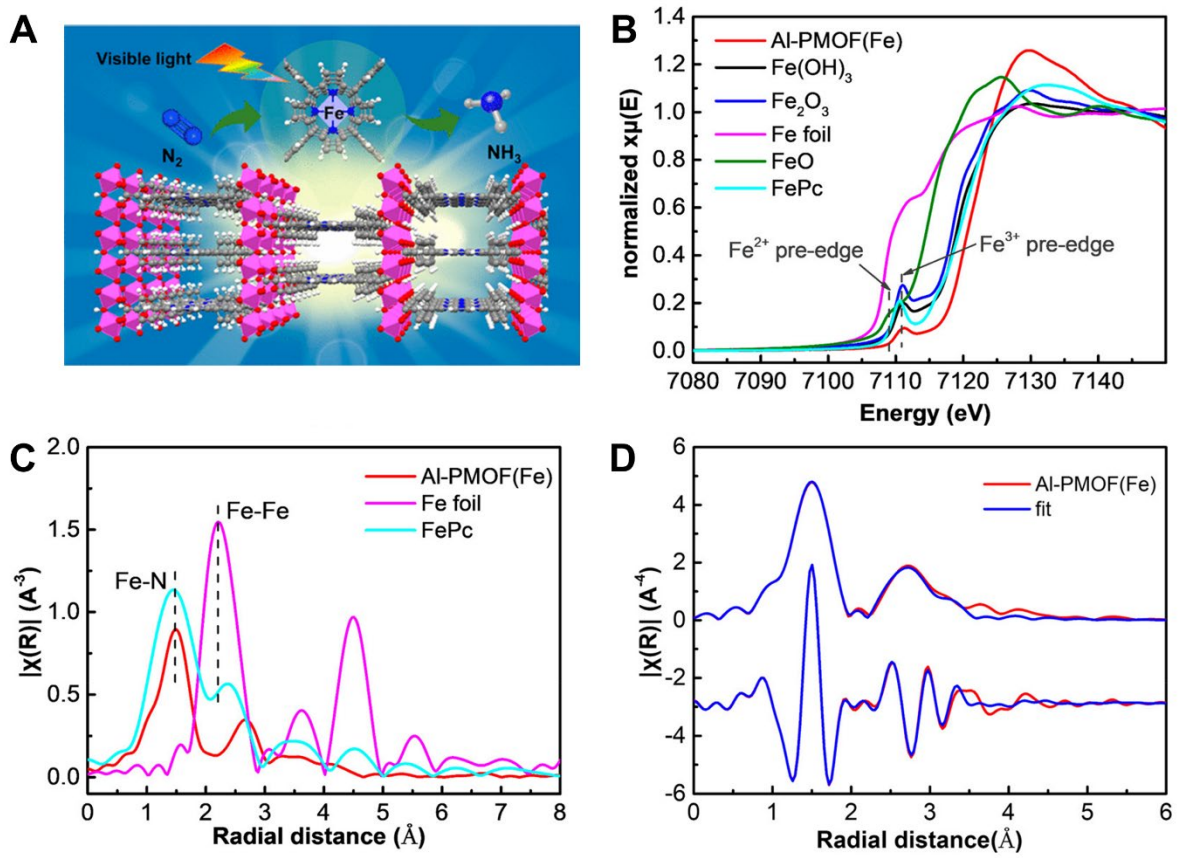

Figure 9. (A) Illustration of NRR on Fe site. (B) Fe K-edge of XANES spectra of MOF sample and references. (C) R-space EXAFS spectra of Fe. (D) Fitting the coordination environment of Fe. Reprinted with permission from ref [54]. Copyright 2021 American Chemical Society.

4.2 PDF: Quantitative insight into the structural coherence of materials by total scattering

While XRD is used to probe the long-range order in MOF, X-ray total scattering and pair distribution functions (PDFs) focus on short- and intermediate-range order and are supplementary to XAS. The X-ray diffusion pattern towards the high scattering vector region can be inversely Fourier transformed to extract the short- and mid-range structure information by offering the probability of finding pairs of atoms separated by a distance r. Therefore, it would be powerful for clarifying the mechanisms of formation or transformation of either linker functionalization, MOF defects, or their metal nodes.[55] Meanwhile, PDF is straightforward to calculate from a known MOF structure and then provide a local-view of material's structure. This mathematical construct subsequently imparts a localized perspective of the material's architectural arrangement, akin to an observer perched upon an atom, surveying the surroundings with a scrutinizing gaze.[56] For example, zirconium and hafnium are notably practical for the design of UiO-66, of which there are over 1300 structures (cluster or part of an extended framework) comprising 3 to 21 Zr or Hf ions in their molecular formulas.[57] PDF can reveal and identify the different phases/topologies of UiO-66 and their cluster structures, as shown in Figure 10.

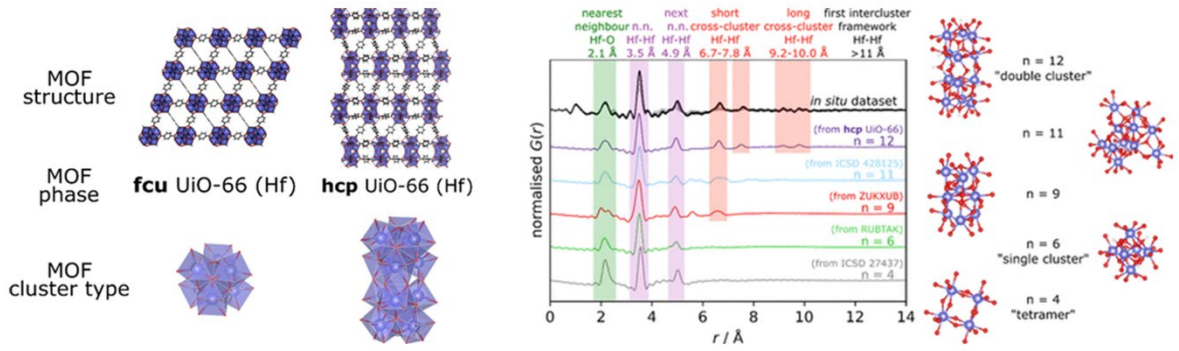

Figure 10. Different phases of UiO-66 and cluster options with their simulated PDF patterns. Reprinted with permission from ref [57]. Copyright 2021 American Chemical Society.

PDF overcomes the limit of X-ray diffraction where a long-range regularity is required to retrieve structural information, making it particularly useful for probing local structures. Currently, the application of PDF for MOF study is still relatively rare, mostly due to the complexity of structural fitting, the complexity of the interfacial bonding, and the difficulty in achieving sufficiently high-resolution PDF patterns. In spite of the fact that the application of PDF to MOFs is a current challenge in the MOF field, we remain convinced that PDF will bring many unexpected structural discoveries in the next few years to the field of MOF materials devoid of long-range ordering.[58]

4.3 Thz/FarIR: Probing metal bond and inorganic cluster

Terahertz/far-infrared (THz/far-IR) is an effective method for investigating the quasi-localized characteristics and collecting chemical bond properties of MOF composite. The *in-situ* THz/far-IR test can further collect information during the formation of composites in MOFs. Our group first applied this technique to reveal the dynamic behaviors of glassy MOF and perovskite composite during sintering. The formation of Zn-I bond at the interface between $CsPbI_3$ perovskite and ZIF-62 MOF glass upon heating was identified (Figure 11A).[52] In another work, our group employed this technique to monitor the metal-N bonding environment in modified ZIF-62(Co).[41] The broad Co-N peak at ca. 334 cm^{-1} of a_gZIF-62(Co)-Fe consistent with structure amorphization, whereas the newly-emerged peak at ca. 344 cm^{-1} indicates the stretching vibration of formed Fe−N (Figure 11B). Moreover, it can also monitor the dynamic behavior of an inorganic component, for example, to identify metal cluster formation and inorganic perovskite phase change.

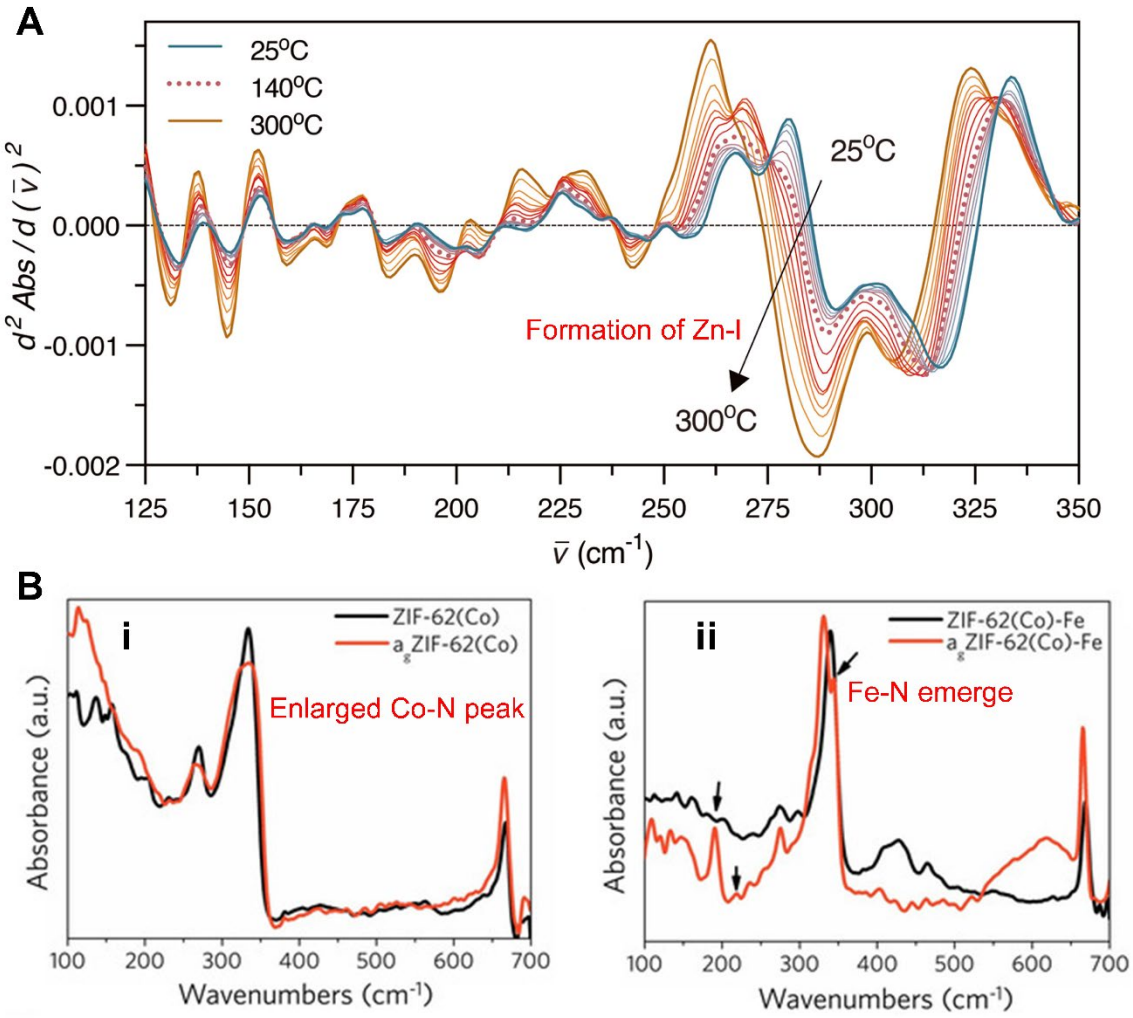

Figure 11. (A) In situ THz FarIR for monitoring Zn-I formation. Reprinted with permission from ref [52]. Copyright 2021 AAAS. (B) ZIF-62(Co)-Fe before and after sintering. (i) Enlarge Co-N peak after sintering. (ii) Fe-N formation after heating. Reprinted with permission from ref [41]. Copyright 2021 Wiley-VCH.

5. Summary and perspective

In conclusion, the utilization of MOF catalysts for the photocatalytic NRR process has demonstrated significant promise as a novel and ideal method for solar energy conversion and value-added chemical production. Moreover, ammonia's stability in aqueous and ease of separation/transportation enable it greater convenience. However, given the low ammonia yield, it should be emphasized that the current lab-scale production has not yet reached meaningful levels as there are still critical obstacles impeding the efficacy of MOF catalysts (The ammonia production over MOFs and other materials are presented at Table 2). Herein, consideration is given to the relevance of major obstacles and the outlook for the future.

Table 2. Summary of ammonia production over photocatalysts

	Catalyst	Ammonia production ($\mu mol \cdot h^{-1} \cdot g^{-1}$)	Reaction condition	Irradiated light (nm)	Reference
1	NH_2-MIL-125(Ti)	12.3	water	>400	[17]

2	U(0.5Hf)-2SH	116.1	K_2SO_3	>420	[32]
3	Cu-MIL-101 (Fe)	315.2	water	Full spectrum	[36]
4	MIL-53(Fe^{II}/Fe^{III})	306	K_2SO_3	>420	[59]
5	ZIF-67@POMs	149	ethanol	Full spectrum	[42]
6	MIL-101(Cr)/ SiW_{12}	75.56	water	Full spectrum	[43]
7	BMOF(Sr)–$_{0.2}$Fe	780	K_2SO_3	Full spectrum	[60]
8	COF_5–Au	427.9	K_2SO_3	Full spectrum	[61]
9	MoS_2	325	water	>420	[62]
10	Bi_2MoO_6	1300	water	>420	[63]

MOF photocatalysts design and modification

Photocatalytic ammonia production by MOF is limited by undesirable conductivity, low light harvesting, and poor photoelectric conversion efficiency due to rapid electron and hole recombination. Therefore, it is important to develop more effective MOF catalysts by rational designing. The light harvesting capacity of MOFs can be improved by introducing coloring ligands or linker's post synthetic modification. Anchoring photosensitizer on ligands can also result in a wider spectrum response. These can considerably increase the density of photogenerated electrons and facilitate the "linker-to-metal charge transfer". Defect engineering such as metal doping or amorphization are growing topics especially in photocatalysis application, despite the fact that a substantive understanding of MOF defects is still obscure and elusive. Other defect engineering techniques, such as introducing vacancy, void, or producing disorder/dislocation, should also be investigated for the NRR of MOF catalysts.[64] Compositing with POM and Plasmonic nanoparticles can also expand light absorption and promote charge separation, as these techniques improve conductivity and facilitate "metal to metal charge transfer"; additionally, MOF's incorporation with perovskite can easily achieve a type II energy band alignment and facilitate majority carriers' separation at their interfaces, as driven by the built-in electric field.[53] Furthermore, in terms of microstructure, the pore of 3D MOF catalysts should not impede the diffusion of nitrogen, ensuring that electrons can transfer from metal sites to nitrogen molecules, whereas 2D MOFs, which typically exhibit a sheet-like structure, should be designed with potential axially unsaturated metal sites with desirable redox activity for efficient NRR process. Another important design factor to consider is light penetration to ensure full utilization of the photocatalyst, where the morphological structure, size and porosity of MOF are key. For example, the construction of MOF nanosheets, which are spatially oriented to avoid stacking,[65] on a 3D substrate can improve light penetration.[66] Moreover, the use of small sized (nanometer) MOF photocatalysts can also contribute to enhanced light penetration.[67] In addition, high porosity MOFs like MIL-125-NH_2 can also allow for easy penetration of light compared to conventional solid metal-oxide photocatalysts, which can lead to enhanced photocatalytic performance.[67, 68]

Operando characterization & DFT calculation facilitate mechanism comprehension

Further studies should be directed at the photocatalytic mechanisms and selectivity of NRR in MOFs. Considering competitive reactions may contribute to product complexity and diversity, coupling DFT calculations for catalyst design with experimental results would aid in the comprehension of reaction intermediates in MOF catalyzed NRR. Moreover, DFT calculations could also provide insight into activation energies and NRR pathway. Understanding the NRR

mechanism is also heavily dependent on characterization techniques. As there are potential existence of complex intermediates with a short life during photocatalytic NRR process, the capture and characterization of these intermediates during the photocatalytic NRR process rely heavily on in situ characterization techniques. Probing the intermediates offers insight into reaction pathway and active site, which are significant for mechanism understanding and catalyst design. In situ Electron Paramagnetic Resonance, Raman, operando XAS, IR, and in situ Thz/FarIR are all effective ways for probing the intermediates, it is strongly suggested that researchers should exploit these advanced techniques.

Optimise experimental conditions and detection methods

Experimental conditions such as chemical reagents, ambient ammonia, and photocatalyst contaminations have a significant impact on the precision of ammonia analysis in a typical suspension aqueous system. Spectrophotometry such as Nessler's reagent method, salicylate method and indophenol blue method are the frequently used methods for ammonia determination, yet they are also prone be affected by the pH of the aqueous phase, the presence of certain metal ions as well as the introduction of sacrificial or nitrogen-containing reagents.[69] To assure the credibility of the results, ion chromatography and nuclear magnetic resonance are strongly recommended. In addition, since amino-functionalized ligands are extensively used with MOFs, the stability of MOFs during NRR should be given additional consideration. Currently, reported cycling tests are fairly short compared to those conducted on an industrial scale. Prolonged irradiation of MOF photocatalysts may result in the degradation of organic linkers, and hence the photocatalytic sites, that can lead to a decrease in its activity over time.[70] This has been investigated for several MOFs containing aromatic carboxylates as ligands such as UiO-66, MIL-101 and MIL-125, where exposure to UV/Vis irradiation over a period of 19 days resulted in ligand decomposition as detected by CO_2 gas evolution.[70] Therefore, long-term monitoring is essential for a better comprehension of the behaviour of catalysts.

MOF photocatalysts synthesis and assembly

The scalable synthesis of MOF catalysts should also be considered. Solvothermal or hydrothermal processes continue to be the most prevalent strategies for synthesizing MOFs. However, this consumes a lot of organic solvents such as DMF, ethanol and methanol. Mechanochemical methods should be further explored as they exhibit rapid reaction kinetics, high productivity, and high repeatability with little to no solvent wastage. Additionally, efforts should be made to optimize the photocatalytic reaction system/reactor, especially the assembling of MOF catalysts. Typically, photocatalytic NRR is conducted in a suspension aqueous system, with some separation issues and yield inhibition at the MOFs catalyst surface. A three-phase reaction system which involves gas-membrane-solution should be highlighted as it can eliminate concentration polarization and bring a high N_2 concentration at the surface of MOF catalyst. Moreover, it reduces the difficulty of product separation. In an industrial viewpoint, to avoid back reaction such as ammonia oxidization upon irradiation, the assembled batch reactor could also integrated with pervaporation membranes for ammonia collection.[71]

In all, due to the nearly unlimited collection of organic ligands and metal nodes, there are many more possible MOFs structures for us to investigate. Meanwhile, MOFs are intermediate between organic and inorganic as well as homo and heterogeneous catalysts, enabling us to draw inspiration not solely from the field of MOFs, yet also from interdisciplinary fields. With a fundamental comprehension of the NRR mechanism and the physiochemical properties of

MOFs, we anticipate this review will spark inspiration for the design of remarkably effective and stable MOF catalysts for nitrogen fixation.

Acknowledgment

The authors acknowledged the financial support from Australian Research (FT210100589). W. Huang acknowledged the UQ Research Training Scholarship.

Declaration of Competing Interest

The authors declare no conflict of interest.

References

1. Chen, J. G.; Crooks, R. M.; Seefeldt, L. C.; Bren, K. L.; Bullock, R. M.; Darensbourg, M. Y.; Holland, P. L.; Hoffman, B.; Janik, M. J.; Jones, A. K., Beyond fossil fuel–driven nitrogen transformations. *Science* **2018,** *360* (6391), eaar6611.
2. Chatterjee, S.; Parsapur, R. K.; Huang, K.-W., Limitations of ammonia as a hydrogen energy carrier for the transportation sector. *ACS Energy Letters* **2021,** *6* (12), 4390-4394.
3. Verleysen, K.; Parente, A.; Contino, F., How sensitive is a dynamic ammonia synthesis process? Global sensitivity analysis of a dynamic Haber-Bosch process (for flexible seasonal energy storage). *Energy* **2021,** *232*, 121016.
4. Gao, Q.; Xu, J.; Bu, X.-H., Recent advances about metal–organic frameworks in the removal of pollutants from wastewater. *Coord. Chem. Rev.* **2019,** *378*, 17-31.
5. Huang, Y.-B.; Liang, J.; Wang, X.-S.; Cao, R., Multifunctional metal–organic framework catalysts: synergistic catalysis and tandem reactions. *Chem. Soc. Rev.* **2017,** *46* (1), 126-157.
6. Farha, O. K.; Hupp, J. T., Rational design, synthesis, purification, and activation of metal–organic framework materials. *Acc. Chem. Res.* **2010,** *43* (8), 1166-1175.
7. Jiao, L.; Seow, J. Y. R.; Skinner, W. S.; Wang, Z. U.; Jiang, H.-L., Metal–organic frameworks: Structures and functional applications. *Mater. Today* **2019,** *27*, 43-68.
8. Xu, C.; Fang, R.; Luque, R.; Chen, L.; Li, Y., Functional metal–organic frameworks for catalytic applications. *Coord. Chem. Rev.* **2019,** *388*, 268-292.
9. Hu, K. Q.; Huang, Z. W.; Zhang, Z. H.; Mei, L.; Qian, B. B.; Yu, J. P.; Chai, Z. F.; Shi, W. Q., Actinide‐Based Porphyrinic MOF as a Dehydrogenation Catalyst. *Chemistry–A European Journal* **2018,** *24* (63), 16766-16769.
10. Xu, S.; Chansai, S.; Stere, C.; Inceesungvorn, B.; Goguet, A.; Wangkawong, K.; Taylor, S. R.; Al-Janabi, N.; Hardacre, C.; Martin, P. A., Sustaining metal–organic frameworks for water–gas shift catalysis by non-thermal plasma. *Nature Catalysis* **2019,** *2* (2), 142-148.
11. Zhang, Q.; Jin, Y.; Ma, L.; Zhang, Y.; Meng, C.; Duan, C., Chromophore‐Inspired Design of Pyridinium‐Based Metal–Organic Polymers for Dual Photoredox Catalysis. *Angew. Chem. Int. Ed.* **2022,** *61* (37), e202204918.
12. Huang, Z.-W.; Hu, K.-Q.; Mei, L.; Wang, C.-Z.; Chen, Y.-M.; Wu, W.-S.; Chai, Z.-F.; Shi, W.-Q., Potassium ions induced framework interpenetration for enhancing the stability of uranium-based porphyrin MOF with visible-light-driven photocatalytic activity. *Inorganic Chemistry* **2020,** *60* (2), 651-659.
13. Wang, Q.; Astruc, D., State of the art and prospects in metal–organic framework (MOF)-based and MOF-derived nanocatalysis. *Chem. Rev.* **2019,** *120* (2), 1438-1511.
14. Sun, X.; Yuan, K.; Zhang, Y., Advances and prospects of rare earth metal-organic frameworks in catalytic applications. *Journal of Rare Earths* **2020,** *38* (8), 801-818.
15. Li, D.; Xu, H.-Q.; Jiao, L.; Jiang, H.-L., Metal-organic frameworks for catalysis: State of the art, challenges, and opportunities. *EnergyChem* **2019,** *1* (1), 100005.

16. Wang, J.; He, C.; Huo, J.; Fu, L.; Zhao, C., A theoretical evaluation of possible N2 reduction mechanism on Mo2B2. *Advanced Theory and Simulations* **2021,** *4* (5), 2100003.
17. Huang, H.; Wang, X.-S.; Philo, D.; Ichihara, F.; Song, H.; Li, Y.; Li, D.; Qiu, T.; Wang, S.; Ye, J., Toward visible-light-assisted photocatalytic nitrogen fixation: A titanium metal organic framework with functionalized ligands. *Applied Catalysis B: Environmental* **2020,** *267*, 118686.
18. Hill, R.; Rinker, R.; Wilson, H. D., Atmospheric nitrogen fixation by lightning. *J. Atmos. Sci.* **1980,** *37* (1), 179-192.
19. Seefeldt, L. C.; Hoffman, B. M.; Dean, D. R., Mechanism of Mo-dependent nitrogenase. *Annual review of biochemistry* **2009,** *78*, 701-722.
20. Huang, W.; Zulkifli, M. Y. B.; Chai, M.; Lin, R.; Wang, J.; Chen, Y.; Chen, V.; Hou, J. In *Recent advances in enzymatic biofuel cells enabled by innovative materials and techniques*, Exploration, Wiley Online Library: 2023; p 20220145.
21. Liang, J.; Burris, R. H., Hydrogen burst associated with nitrogenase-catalyzed reactions. *Proceedings of the national Academy of Sciences* **1988,** *85* (24), 9446-9450.
22. Thorneley, R. N.; Lowe, D. J., Kinetics and mechanism of the nitrogenase enzyme system. *Molybdenum enzymes* **1985,** *7*, 89-116.
23. Van der Ham, C. J.; Koper, M. T.; Hetterscheid, D. G., Challenges in reduction of dinitrogen by proton and electron transfer. *Chem. Soc. Rev.* **2014,** *43* (15), 5183-5191.
24. Hou, J.; Yang, M.; Zhang, J., Recent advances in catalysts, electrolytes and electrode engineering for the nitrogen reduction reaction under ambient conditions. *Nanoscale* **2020,** *12* (13), 6900-6920.
25. Xia, P.; Pan, X.; Jiang, S.; Yu, J.; He, B.; Ismail, P. M.; Bai, W.; Yang, J.; Yang, L.; Zhang, H., Designing a redox heterojunction for photocatalytic "overall nitrogen fixation" under mild conditions. *Adv. Mater.* **2022,** *34* (28), 2200563.
26. Liu, C.; Hao, D.; Ye, J.; Ye, S.; Zhou, F.; Xie, H.; Qin, G.; Xu, J.; Liu, J.; Li, S., Knowledge-Driven Design and Lab-Based Evaluation of B-doped TiO2 Photocatalysts for Ammonia Synthesis. *Advanced energy materials* **2023,** *13* (8), 2204126.
27. Zhao, Y.; Zheng, L.; Shi, R.; Zhang, S.; Bian, X.; Wu, F.; Cao, X.; Waterhouse, G. I.; Zhang, T., Alkali etching of layered double hydroxide nanosheets for enhanced photocatalytic N2 reduction to NH3. *Advanced energy materials* **2020,** *10* (34), 2002199.
28. Zhang, S.; Zhao, Y.; Shi, R.; Zhou, C.; Waterhouse, G. I.; Wu, L. Z.; Tung, C. H.; Zhang, T., Efficient photocatalytic nitrogen fixation over Cuδ+-modified defective ZnAl-layered double hydroxide nanosheets. *Advanced Energy Materials* **2020,** *10* (8), 1901973.
29. Dhakshinamoorthy, A.; Asiri, A. M.; Garcia, H., Metal–organic framework (MOF) compounds: photocatalysts for redox reactions and solar fuel production. *Angew. Chem. Int. Ed.* **2016,** *55* (18), 5414-5445.
30. Fu, Y.; Sun, D.; Chen, Y.; Huang, R.; Ding, Z.; Fu, X.; Li, Z., An amine-functionalized titanium metal–organic framework photocatalyst with visible-light-induced activity for CO2 reduction. *Angew. Chem. Int. Ed.* **2012,** *51* (14), 3364-3367.
31. Horiuchi, Y.; Toyao, T.; Saito, M.; Mochizuki, K.; Iwata, M.; Higashimura, H.; Anpo, M.; Matsuoka, M., Visible-light-promoted photocatalytic hydrogen production by using an amino-functionalized Ti (IV) metal–organic framework. *The Journal of Physical Chemistry C* **2012,** *116* (39), 20848-20853.
32. An, K.; Ren, H.; Yang, D.; Zhao, Z.; Gao, Y.; Chen, Y.; Tan, J.; Wang, W.; Jiang, Z., Nitrogenase-inspired bimetallic metal organic frameworks for visible-light-driven nitrogen fixation. *Applied Catalysis B: Environmental* **2021,** *292*, 120167.
33. Lin, G.; Zhang, Y.; Hua, Y.; Zhang, C.; Jia, C.; Ju, D.; Yu, C.; Li, P.; Liu, J., Bioinspired Metalation of the Metal-Organic Framework MIL-125-NH2 for Photocatalytic NADH Regeneration and Gas-Liquid-Solid Three-Phase Enzymatic CO2 Reduction. *Angew. Chem. Int. Ed.* **2022,** *61* (31), e202206283.

34. Fang, Z.; Bueken, B.; De Vos, D. E.; Fischer, R. A., Defect-engineered metal–organic frameworks. *Angew. Chem. Int. Ed.* **2015,** *54* (25), 7234-7254.
35. Shi, R.; Zhao, Y.; Waterhouse, G. I.; Zhang, S.; Zhang, T., Defect engineering in photocatalytic nitrogen fixation. *Acs Catalysis* **2019,** *9* (11), 9739-9750.
36. Zhang, Z.; Li, F.; Li, G.; Li, R.; Wang, Y.; Wang, Y.; Zhang, X.; Zhang, L.; Li, F.; Liu, J., Cu-doped MIL-101 (Fe) with enhanced photocatalytic nitrogen fixation performance. *J. Solid State Chem.* **2022,** *310*, 123041.
37. Yan, S.; Zhang, X.; Wu, D.; Yu, Y.; Ding, Z., A system investigation on Ru-MOF-74 with efficient photocatalytic nitrogen fixation performance. *Surfaces and Interfaces* **2022,** *33*, 102225.
38. Gao, W.; Li, X.; Zhang, X.; Su, S.; Luo, S.; Huang, R.; Jing, Y.; Luo, M., Photocatalytic nitrogen fixation of metal–organic frameworks (MOFs) excited by ultraviolet light: insights into the nitrogen fixation mechanism of missing metal cluster or linker defects. *Nanoscale* **2021,** *13* (16), 7801-7809.
39. Guo, B.; Cheng, X.; Tang, Y.; Guo, W.; Deng, S.; Wu, L.; Fu, X., Dehydrated UiO-66 (SH) 2: The Zr− O Cluster and Its Photocatalytic Role Mimicking the Biological Nitrogen Fixation. *Angew. Chem.* **2022,** *134* (13), e202117244.
40. Sun, S.; Song, P.; Cui, J.; Liang, S., Amorphous TiO 2 nanostructures: synthesis, fundamental properties and photocatalytic applications. *Catalysis Science & Technology* **2019,** *9* (16), 4198-4215.
41. Lin, R.; Li, X.; Krajnc, A.; Li, Z.; Li, M.; Wang, W.; Zhuang, L.; Smart, S.; Zhu, Z.; Appadoo, D., Mechanochemically synthesised flexible electrodes based on bimetallic metal–organic framework glasses for the oxygen evolution reaction. *Angew. Chem. Int. Ed.* **2022,** *61* (4), e202112880.
42. Li, X. H.; He, P.; Wang, T.; Zhang, X. W.; Chen, W. L.; Li, Y. G., Keggin-Type Polyoxometalate-Based ZIF-67 for Enhanced Photocatalytic Nitrogen Fixation. *ChemSusChem* **2020,** *13* (10), 2769-2778.
43. Su, S.; Li, X.; Zhang, X.; Zhu, J.; Liu, G.; Tan, M.; Wang, Y.; Luo, M., Keggin-type SiW12 encapsulated in MIL-101 (Cr) as efficient heterogeneous photocatalysts for nitrogen fixation reaction. *J. Colloid Interface Sci.* **2022,** *621*, 406-415.
44. Liu, Y.; Liu, C.-H.; Debnath, T.; Wang, Y.; Pohl, D.; Besteiro, L. V.; Meira, D. M.; Huang, S.; Yang, F.; Rellinghaus, B., Silver nanoparticle enhanced metal-organic matrix with interface-engineering for efficient photocatalytic hydrogen evolution. *Nat. Commun.* **2023,** *14* (1), 541.
45. Zheng, G.; Pastoriza-Santos, I.; Pérez-Juste, J.; Liz-Marzán, L. M., Plasmonic metal-organic frameworks. *SmartMat* **2021,** *2* (4), 446-465.
46. Chen, L.-W.; Hao, Y.-C.; Guo, Y.; Zhang, Q.; Li, J.; Gao, W.-Y.; Ren, L.; Su, X.; Hu, L.; Zhang, N., Metal–organic framework membranes encapsulating gold nanoparticles for direct plasmonic photocatalytic nitrogen fixation. *J. Am. Chem. Soc.* **2021,** *143* (15), 5727-5736.
47. Xing, P.; Wu, S.; Chen, Y.; Chen, P.; Hu, X.; Lin, H.; Zhao, L.; He, Y., New application and excellent performance of Ag/KNbO3 nanocomposite in photocatalytic NH3 synthesis. *ACS Sustainable Chemistry & Engineering* **2019,** *7* (14), 12408-12418.
48. Zhang, H.; Li, X.; Su, H.; Chen, X.; Zuo, S.; Yan, X.; Liu, W.; Yao, C., Sol–gel synthesis of upconversion perovskite/attapulgite heterostructures for photocatalytic fixation of nitrogen. *J. Sol-Gel Sci. Technol.* **2019,** *92*, 154-162.
49. Tao, R.; Li, X.; Li, X.; Shao, C.; Liu, Y., TiO 2/SrTiO 3/gC 3 N 4 ternary heterojunction nanofibers: gradient energy band, cascade charge transfer, enhanced photocatalytic hydrogen evolution, and nitrogen fixation. *Nanoscale* **2020,** *12* (15), 8320-8329.
50. Chamack, M.; Ifires, M.; Akbar Razavi, S. A.; Morsali, A.; Addad, A.; Larimi, A.; Szunerits, S.; Boukherroub, R., Photocatalytic performance of perovskite and metal–organic framework hybrid material for the reduction of N2 to ammonia. *Inorganic Chemistry* **2022,** *61* (3), 1735-1744.
51. Liu, J.; Li, R.; Zu, X.; Zhang, X.; Wang, Y.; Wang, Y.; Fan, C., Photocatalytic conversion of nitrogen to ammonia with water on triphase interfaces of hydrophilic-hydrophobic composite Bi4O5Br2/ZIF-8. *Chem. Eng. J.* **2019,** *371*, 796-803.

52. Hou, J.; Chen, P.; Shukla, A.; Krajnc, A.; Wang, T.; Li, X.; Doasa, R.; Tizei, L. H.; Chan, B.; Johnstone, D. N., Liquid-phase sintering of lead halide perovskites and metal-organic framework glasses. *Science* **2021,** *374* (6567), 621-625.
53. Chen, P.; Hou, J.; Wang, L., Metal-organic framework-tailored perovskite solar cells. *Microstructures* **2022,** *2* (3), 1-15.
54. Shang, S.; Xiong, W.; Yang, C.; Johannessen, B.; Liu, R.; Hsu, H.-Y.; Gu, Q.; Leung, M. K.; Shang, J., Atomically dispersed iron metal site in a porphyrin-based metal–organic framework for photocatalytic nitrogen fixation. *ACS nano* **2021,** *15* (6), 9670-9678.
55. Molina, M. A.; Manjón-Sanz, A.; Sánchez-Sánchez, M., On the contribution of Pair Distribution Function (PDF) to the characterization of nanocrystalline MOFs: The case of M-MOF-74. *Microporous Mesoporous Mater.* **2021,** *319*, 110973.
56. Terban, M. W.; Billinge, S. J., Structural analysis of molecular materials using the pair distribution function. *Chem. Rev.* **2021,** *122* (1), 1208-1272.
57. Firth, F. C.; Gaultois, M. W.; Wu, Y.; Stratford, J. M.; Keeble, D. S.; Grey, C. P.; Cliffe, M. J., Exploring the Role of Cluster Formation in UiO Family Hf Metal–Organic Frameworks with in Situ X-ray Pair Distribution Function Analysis. *J. Am. Chem. Soc.* **2021,** *143* (47), 19668-19683.
58. Castillo-Blas, C.; Moreno, J. M.; Romero-Muñiz, I.; Platero-Prats, A. E., Applications of pair distribution function analyses to the emerging field of non-ideal metal–organic framework materials. *Nanoscale* **2020,** *12* (29), 15577-15587.
59. Zhao, Z.; Yang, D.; Ren, H.; An, K.; Chen, Y.; Zhou, Z.; Wang, W.; Jiang, Z., Nitrogenase-inspired mixed-valence MIL-53 (FeII/FeIII) for photocatalytic nitrogen fixation. *Chem. Eng. J.* **2020,** *400*, 125929.
60. Zhao, Z.; Ren, H.; Yang, D.; Han, Y.; Shi, J.; An, K.; Chen, Y.; Shi, Y.; Wang, W.; Tan, J., Boosting nitrogen activation via bimetallic organic frameworks for photocatalytic ammonia synthesis. *ACS Catalysis* **2021,** *11* (15), 9986-9995.
61. He, T.; Zhao, Z.; Liu, R.; Liu, X.; Ni, B.; Wei, Y.; Wu, Y.; Yuan, W.; Peng, H.; Jiang, Z., Porphyrin-Based Covalent Organic Frameworks Anchoring Au Single Atoms for Photocatalytic Nitrogen Fixation. *J. Am. Chem. Soc.* **2023,** *145* (11), 6057-6066.
62. Sun, S.; Li, X.; Wang, W.; Zhang, L.; Sun, X., Photocatalytic robust solar energy reduction of dinitrogen to ammonia on ultrathin MoS2. *Applied Catalysis B: Environmental* **2017,** *200*, 323-329.
63. Hao, Y.; Dong, X.; Zhai, S.; Ma, H.; Wang, X.; Zhang, X., Hydrogenated bismuth molybdate nanoframe for efficient sunlight‐driven nitrogen fixation from air. *Chemistry–A European Journal* **2016,** *22* (52), 18722-18728.
64. Bai, S.; Zhang, N.; Gao, C.; Xiong, Y., Defect engineering in photocatalytic materials. *Nano Energy* **2018,** *53*, 296-336.
65. Zhao, Y.; Zhang, S.; Shi, R.; Waterhouse, G. I.; Tang, J.; Zhang, T., Two-dimensional photocatalyst design: A critical review of recent experimental and computational advances. *Mater. Today* **2020,** *34*, 78-91.
66. Ding, X.; Liu, H.; Chen, J.; Wen, M.; Li, G.; An, T.; Zhao, H., In situ growth of well-aligned Ni-MOF nanosheets on nickel foam for enhanced photocatalytic degradation of typical volatile organic compounds. *Nanoscale* **2020,** *12* (17), 9462-9470.
67. Zhang, L.; Shi, X.; Zhang, Z.; Kuchel, R. P.; Namivandi‐Zangeneh, R.; Corrigan, N.; Jung, K.; Liang, K.; Boyer, C., Porphyrinic Zirconium Metal–Organic Frameworks (MOFs) as Heterogeneous Photocatalysts for PET‐RAFT Polymerization and Stereolithography. *Angewandte Chemie International Edition* **2021,** *60* (10), 5489-5496.
68. Kampouri, S.; Nguyen, T. N.; Ireland, C. P.; Valizadeh, B.; Ebrahim, F. M.; Capano, G.; Ongari, D.; Mace, A.; Guijarro, N.; Sivula, K., Photocatalytic hydrogen generation from a visible-light responsive metal–organic framework system: the impact of nickel phosphide nanoparticles. *Journal of Materials Chemistry A* **2018,** *6* (6), 2476-2481.

69. Zhao, Y.; Shi, R.; Bian, X.; Zhou, C.; Zhao, Y.; Zhang, S.; Wu, F.; Waterhouse, G. I.; Wu, L. Z.; Tung, C. H., Ammonia detection methods in photocatalytic and electrocatalytic experiments: how to improve the reliability of NH3 production rates? *Advanced Science* **2019,** *6* (8), 1802109.
70. Mateo, D.; Santiago‐Portillo, A.; Albero, J.; Navalón, S.; Alvaro, M.; García, H., Long‐Term Photostability in Terephthalate Metal–Organic Frameworks. *Angewandte Chemie* **2019,** *131* (49), 18007-18012.
71. Zhao, Y.; Miao, Y.; Zhou, C.; Zhang, T., Artificial photocatalytic nitrogen fixation: Where are we now? Where is its future? *Molecular Catalysis* **2022,** *518*, 112107.

ToC

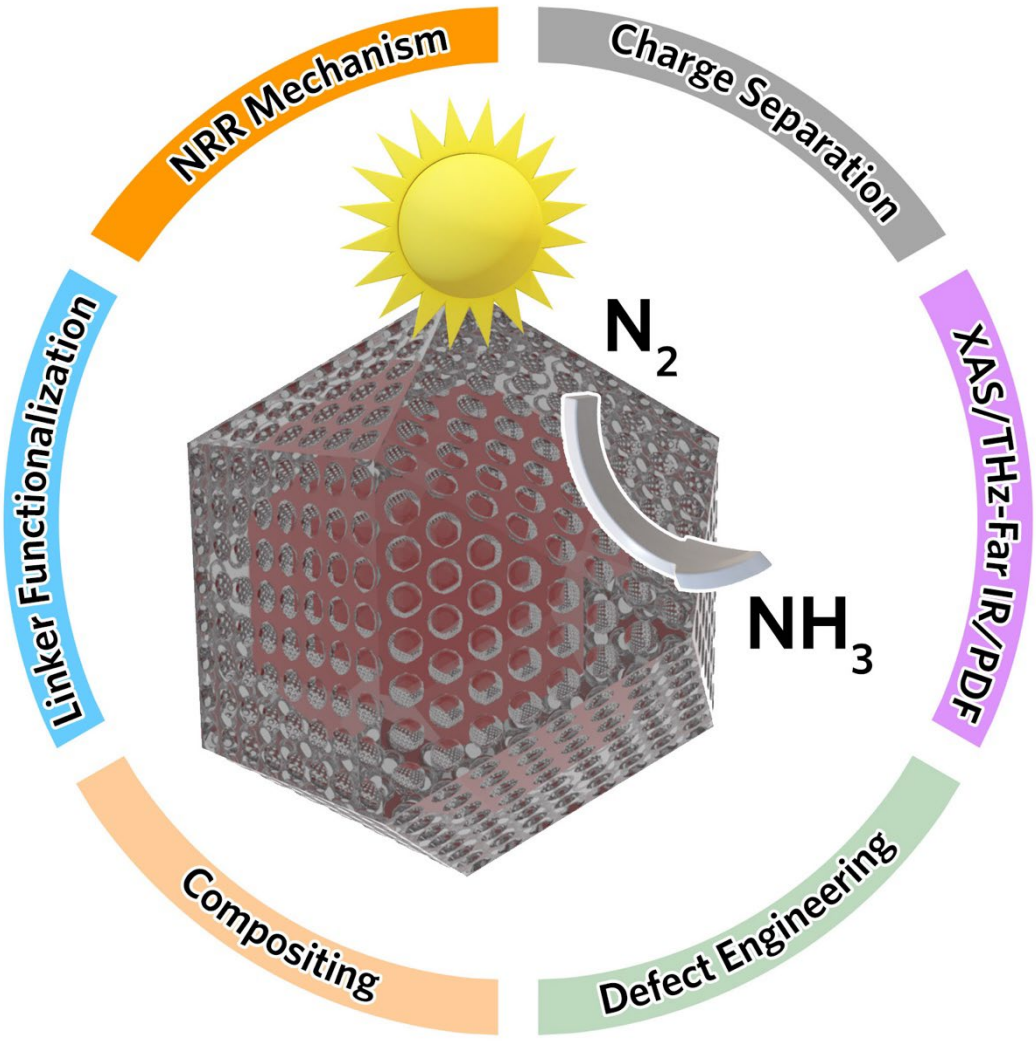

Author bio:

Dr Jingwei Hou received his Ph.D. in Chemical Engineering from the University of New South Wales in 2015. He then joined the UNESCO Centre for Membrane Science and Technology (2015-2017) and University of Cambridge (2017-2019, affiliate of the Trinity College) for this post-doctoral research. In 2019, he returned Australia as an ARC DECRA Fellow at the School of Chemical Engineering, University of Queensland. In 2021, he was named the ARC Future Fellow. He is currently a Senior Lecturer and group leader of the Functional Materials Engineering (fme) Lab.